MASS FLOW RATE INDUCED BY COMBINED ROOF SOLAR COLLECTOR AND VERTICAL STACK IN A HOT HUMID CLIMATE

Wardah Fatimah Mohammad Yusoff,[1]* Abdul Razak Sapian,[2] Elias Salleh,[3]
Nor Mariah Adam,[4] and Zabidi Hamzah[1]

ABSTRACT

This paper presents the investigation of solar induced ventilation that utilizes roof solar collector and vertical stack. Three prototypes, namely A, B and C, were developed based on preliminary experimental work. They were then used in simulation study with the objective of determining the prototype that was able to induce the highest mass flow rate. The validation of simulation modelling against experiment indicated a good agreement between these two results. The findings showed that prototype A induced the highest mass flow rate. However, prototype C, which had obstructions at the stack outlets, was more appropriate for application in Malaysia due to various prevailing wind directions. In addition, the findings also indicated that besides solar radiation, the mass flow rate induced by the prototypes was also influenced by the local wind direction, the inlet and outlet positions as well as the outlet design. In summary, the findings highlighted the potential application of the proposed solar induced ventilation in a hot and humid climate.

KEYWORDS

solar induced ventilation, roof solar collector, vertical stack, mass flow rate, hot humid climate, simulation modelling

1. INTRODUCTION

The increase of global warming and climate change issues has encouraged the development of green technologies in recent years. These technologies mostly utilize natural resources, such as wind, solar and biomass. In a hot and humid climate, the copious solar irradiation throughout the year provides great potential for solar technologies. One of them is solar induced ventilation, which utilizes buoyancy forces to create air movement.

[1]Department of Architecture, Faculty of Engineering and Built Environment, Universiti Kebangsaan Malaysia, Malaysia.
[2]Department of Architecture, Kulliyyah of Architecture and Environmental Design, International Islamic University Malaysia, Malaysia.
[3]Solar Energy Research Institute, Universiti Kebangsaan Malaysia, Malaysia.
[4]Department of Mechanical and Manufacturing Engineering, Faculty of Engineering, Universiti Putra Malaysia, Malaysia.
*Corresponding author: tel:+6019-6355295; fax:+603-89118302; email address: wardahyusoff@gmail.com

Downloaded from https://prime-pdf-watermark.prime-prod.pubfactory.com/ at 2025-08-29 via free access

The basic concept of solar induced ventilation is that the absorber wall or plate is heated by solar radiation. The convective heat transfer from the absorber to the air results in higher air temperature inside the stack or cavity. The decrease in the air density due to the increase in the temperature causes the air to rise. The heated air is then replaced by the cooler air from the attached space (Awbi, 2003; Harris & Helwig, 2007). Normally, a solar induced ventilation consists of three main components, which are a glass cover, an air cavity, and an absorber wall or plate. The heat transfer processes in a solar induced ventilation comprise solar radiation incidence and absorption in the glass cover and absorber wall/plate, conductive heat transfer through the glass cover and absorber wall/plate, radiative heat transfer between the absorber surface and the glass surface, convective heat transfer between the internal surfaces and the air inside the cavity, convective heat transfer due to wind over the glass cover as well as radiative heat transfer between the glass cover and the sky (Bansal, Mathur, Mathur, & Jain, 2005; Bassiouny & Koura, 2008; Mathur, Mathur, & Anupma, 2006b).

Over the past century, solar induced ventilation strategies in a hot and humid climate have been studied by many researchers (Table 1). The strategies are able to enhance the stack effect ventilation due to the presence of heat from the solar irradiation, which increases the air temperature difference between the inside and outside of the stack. Hence, it promotes natural ventilation, thus encouraging energy savings in buildings. Moreover, the strategies can also be applied to enhance the thermal comfort in buildings. Thermal comfort is influenced by six main factors, which are air temperature, mean radiant temperature, humidity, air movement, clothing and metabolic rate (Boutet, 1987). However, besides higher air velocity, numerous air changes per hour (ACH) can also improve the thermal comfort in a humid climate (Hamdy & Fikry, 1998). The increase in ACH can be achieved via the utilization of solar induced ventilation strategies. Furthermore, the strategies that enhance stack effect ventilation can also provide a cooling effect in a climate where the wind is very calm, as well as when a building's access to wind is impeded by the surrounding condition (Brown & DeKay, 2001).

The investigations of the proposed strategy under the actual climatic conditions in Malaysia showed that it was possible to create a significant temperature difference between the stack air and the ambient air. The highest air temperature difference of 9.9 °C was obtained for 877 W/m^2 solar radiation (Yusoff, Salleh, Adam, Sapian, & Yusof Sulaiman, 2010). This air temperature difference is more than the usual air temperature difference achieved by stack ventilation in Malaysian naturally ventilated buildings, which is less than 5 °C (Kubota, Chyee, & Ahmad, 2009; A. M. Nugroho, Hamdan, M., & Ossen, D.R. , 2007).

The solar induced ventilation strategies that have been investigated are Trombe wall, solar chimney, and roof solar collector. A roof solar collector is the most studied strategy in the hot and humid climate, as shown in Table 1. This is due to its potential in collecting more solar radiation when the solar altitude is high, compared to a Trombe wall and a solar chimney (Awbi, 2003; Mathur, et al., 2006b). However, the drawback of a roof solar collector is the stack height, which is restricted by the roof slope (Awbi, 2003; Harris & Helwig, 2007). Khedari et al. (2000a) emphasized that the ACH induced by a roof solar collector alone is still insufficient for occupant comfort. The induced ACH of a roof solar collector examined by Khedari et al. (2000a) was 4-5 ACH. It was far below the required ACH for occupant comfort, which was 20 ACH. Therefore, in enhancing the stack height, it is proposed that a roof solar collector is used together with a vertical stack. The roof solar collector functions in collecting solar radiation, whilst the vertical stack provides a significant stack height for sufficient stack pressure (Yusoff, et al., 2010).

Downloaded from https://prime-pdf-watermark.prime-prod.pubfactory.com/ at 2025-08-29 via free access

TABLE 1. The solar induced ventilation studies in a hot and humid climate.

Research	Year	Building				Strategy			Output performance			
		Office/multi-storey building	Institutional	Commercial / Industrial	Residential/Room	Trombe Wall (TW)	Solar chimney (SC)	Roof solar collector (RSC)	Air Velocity	Air Flow Rate	ACH	Temperature
Bansal et al.	(1994)							*		*		*
Rahman	(1994)				*			*	*	*	*	*
Khedari et al.	(1997)				*			*	*	*		
Hirunlabh et al	(1999)				*	*				*		*
Khedari et al.	(2000b)		*			*		*	*		*	*
Khedari et al.	(2000a)				*			*		*	*	
Hirunlabh et al.	(2001)				*			*		*		
Khedari et al.	(2003)				*	*		*		*		*
Ong and Chow	(2003)				*	*			*	*		*
Bansal et al.	(2005)				*	*			*			*
Mathur et al.	(2006b)				*			*		*		
Mathur et al.	(2006a)				*	*				*	*	
Chantawong et al.	(2006)				*	*			*			*
Nugroho	(2007)				*		*		*	*		*
Puangsombut et al.	(2007)							*		*		
Chungloo & Limmeechokchai	(2007)				*			*		*	*	*
Arce et al.	(2009)						*			*		*
Chungloo & Limmeechokchai	(2009)				*			*	*	*		*
Punyasompun et al	(2009)	*				*				*		*
Yusoff et al.	(2010)							*	*			*
Ong	(2011)							*				*

The present study is an extension of the work by Yusoff et al. (2010). The research indicated that the proposed solar induced ventilation was able to enhance the stack ventilation in the hot and humid climate of Malaysia. Analyses were executed on three solar induced ventilation prototypes, namely A, B and C. However, it was difficult to compare and decide on the prototype that induced the highest mass flow rate, as the measurements were executed on different days. There was variability in the environmental data between the days as they were conducted under the actual environmental conditions (Yusoff, et al., 2010). Moreover, an experiment has limitations in the provision of visual graphic representation, which is essential in analyzing the air flow pattern inside the prototypes. Hence, the aim of this paper is to assess the mass flow rate induced by the proposed strategy in a hot and humid climate

Downloaded from https://prime-pdf-watermark.prime-prod.pubfactory.com/ at 2025-08-29 via free access

using simulation modelling technique. A simulation modelling technique was employed in this research as it enables the control of environmental conditions for ease of comparing the prototypes. Moreover, it also provides a visual graphic representation.

2. THE PROPOSED STRATEGY

The proposed solar induced ventilation strategy comprises two zones, which are roof solar collector and vertical stack (Figure 1). The roof solar collector functions in collecting solar radiation, whilst the vertical stack provides a significant stack height for sufficient stack pressure. The air temperature difference, hence the density difference exists between these two zones. This is due to the heating of air in the roof solar collector only, whilst the vertical stack functions as a conventional chimney, with no collection of solar radiation. Therefore, the heated air inside the roof solar collector's cavity rises and flows into the vertical stack. The hot air then flows out via the outlet at the top of the vertical stack, whilst cooler air is drawn into the proposed strategy via an inlet at the bottom.

3. METHODOLOGY

3.1 Simulation Modelling

The methodology employed was simulation modelling using Computational Fluid Dynamic (CFD) software, FloVENT version 9.1. The feasibility of FloVENT had been proven by Manz (2003) who had employed FloVENT version 3.1 in examining the Nusselt numbers for natural convection. In the present research, three prototypes namely A, B and C were developed. Prototype A was the base model in which its configuration and dimensions were derived from the literature (Yusoff, et al., 2010). Prototype B and C were the subsequent modifications of prototype A. Figure 2 depicts the configurations and dimensions of these prototypes. Basically, they were similar except in the design of the vertical stack outlet. Prototype A had an outlet at one side of the vertical stack walls, whereas prototype B had outlets at two sides of the walls. The outlets of prototype C were similar to the prototype B, but with addition of obstructions at a distance of 0.15 m from the outlets. The roof solar collector had a dimension

FIGURE 1. The proposed solar induced ventilation.

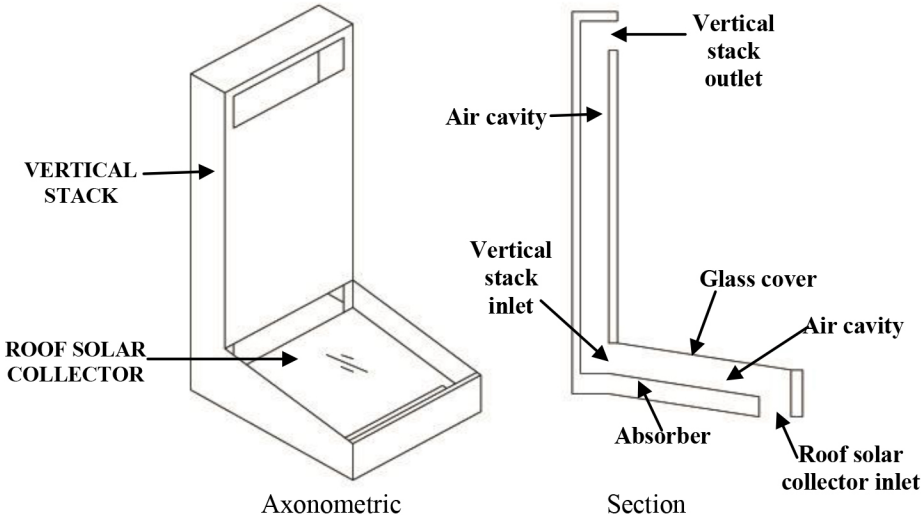

Downloaded from https://prime-pdf-watermark.prime-prod.pubfactory.com/ at 2025-08-29 via free access

FIGURE 2. Sections of prototype A (a), B (b) and C (c).

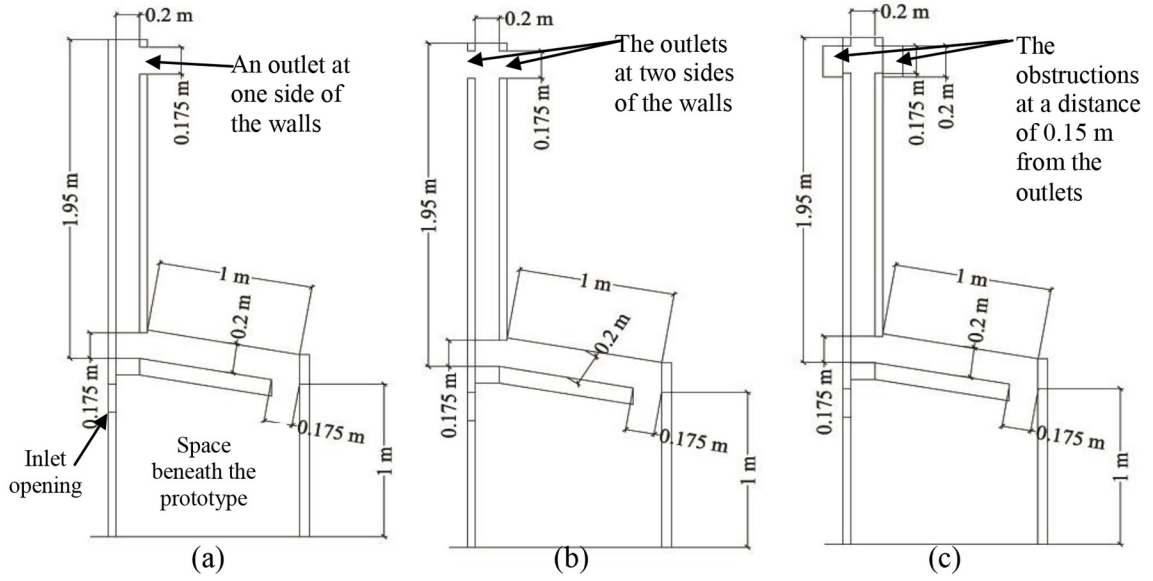

of 1 m (width) × 1 m (length) × 0.2 m (cavity width), whilst for the vertical stack, the dimensions were 1 m (width) × 1.95 m (height) × 0.2 m (cavity width). The materials assigned to the prototypes were also made as similar as possible to the prototypes in the experiment by Yusoff et al. (2010). Moreover, the prototypes were also positioned at 1 m above the ground level in the experiment. The space beneath it was covered to reduce the wind effects. However, there was an opening at one of the covers to allow air movement into the prototypes (Yusoff, et al., 2010). Hence, the similar condition was applied in the simulation modelling, as shown in Figure 2.

The prototype was placed in a 7 m (length) × 7 m (width) × 6 m (high) solution domain (Figure 3). It was oriented towards north. The simulations used a steady state and three dimensional flow analysis. The compared variable was mass flow rate that was derived by multiplying air velocity data with air density and a cross sectional area where the air flowed through.

FIGURE 3. The position of the prototype in the overall solution domain.

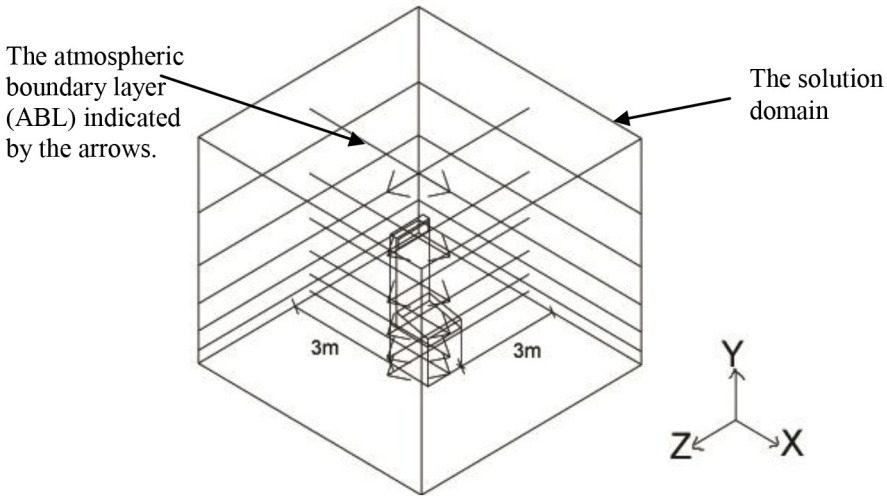

Downloaded from https://prime-pdf-watermark.prime-prod.pubfactory.com/ at 2025-08-29 via free access

Hence, the monitor points were placed at three locations, which were the inlet, middle and outlet of the vertical stack (Figure 4).

FIGURE 4. The location of monitor points in the prototype.

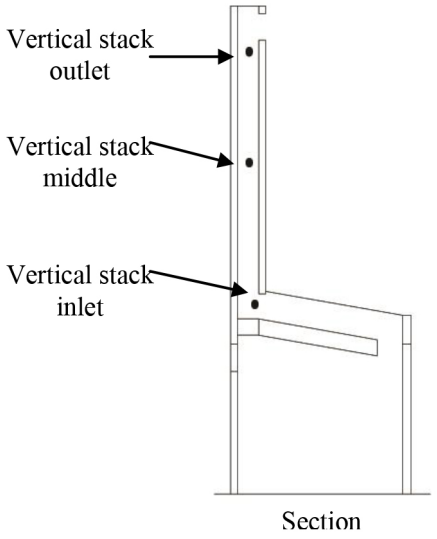

The flow regime was considered turbulent, in which the LVEL K-Epsilon turbulence model was used. This turbulence model utilizes k-ε (turbulent kinetic energy (k) and turbulent dissipation rate (ε)) approach in the calculation (MentorGraphics, 2010). The solar radiation calculation was activated, in which the required input data were site latitude, simulation day, solar time and solar intensity. The simulations also considered wind effects by applying Atmospheric Boundary Layer (ABL), which was downloaded from the FLOVENT website

Besides the general setting-up, the simulations also employed Cartesian grid system. A spatial solution grid was utilized where the solution domain was divided into grid cells. The conservation equations were calculated in each grid cell. The number of grid cells influences the accuracy of the result. Finer and more numbers of grid cells provide more accurate results, but higher computation time (MentorGraphics, 2010). Hence, in the simulations, the grid started with coarse grid from the boundary of the solution domain and became finer when approaching the studied model. Grid constraint was applied at the prototype and focused area of building model. The grid constraint allows the control of amount and size of grid cells at the particular area (MentorGraphics, 2010).

The environmental parameters applied for the initial boundary conditions were the measured environmental data of the experiment by Yusoff et al. (2010). The experiment was executed for eight days, in which the days were classified into two categories, namely the days with semi-clear sky condition and the days with overcast sky condition. The environmental data employed for the simulations were the average data of the days with semi-clear sky condition. The simulation durations were from 9 a.m. to 4 p.m., where the average value of each environmental parameter for every hour was utilized. The wind directions were from the south, southeast and southwest, which were similar to the directions in the experiment by Yusoff et al. (2010). Another simulation was made for wind direction from the north. The purpose was to determine the effects of wind direction on the induced mass flow rate of the prototypes.

3.2 Validation of Simulation Modelling

In the present study, the simulation modelling was validated against the experiment by Yusoff et. al. (2010). The variables compared for the validation were air temperature and air velocity. The air temperature was compared at six measurement point locations, namely the RSC inlet, RSC 1, RSC 2, vertical stack inlet, vertical stack middle and vertical stack outlet (Figure 5). Meanwhile, the air velocity was compared at three measurement point locations which were the RSC inlet, vertical stack inlet and vertical stack outlet.

Figures 6 and 7 depict the deviation percentage at each measurement point location. The presented values were the average values from 9 a.m. to 4 p.m. The validation of the simulation modelling against the experiment indicated a good agreement between these two results.

Downloaded from https://prime-pdf-watermark.prime-prod.pubfactory.com/ at 2025-08-29 via free access

FIGURE 5. The six locations of air temperature measurement points.

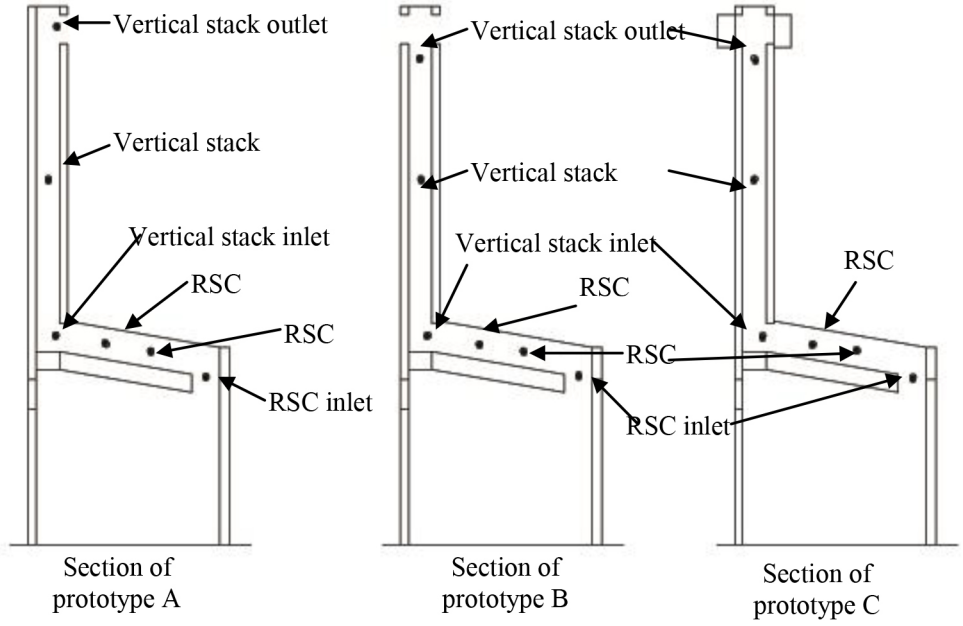

FIGURE 6. The average percentage of deviations for air temperature at six measurement point locations for prototype A, B and C.

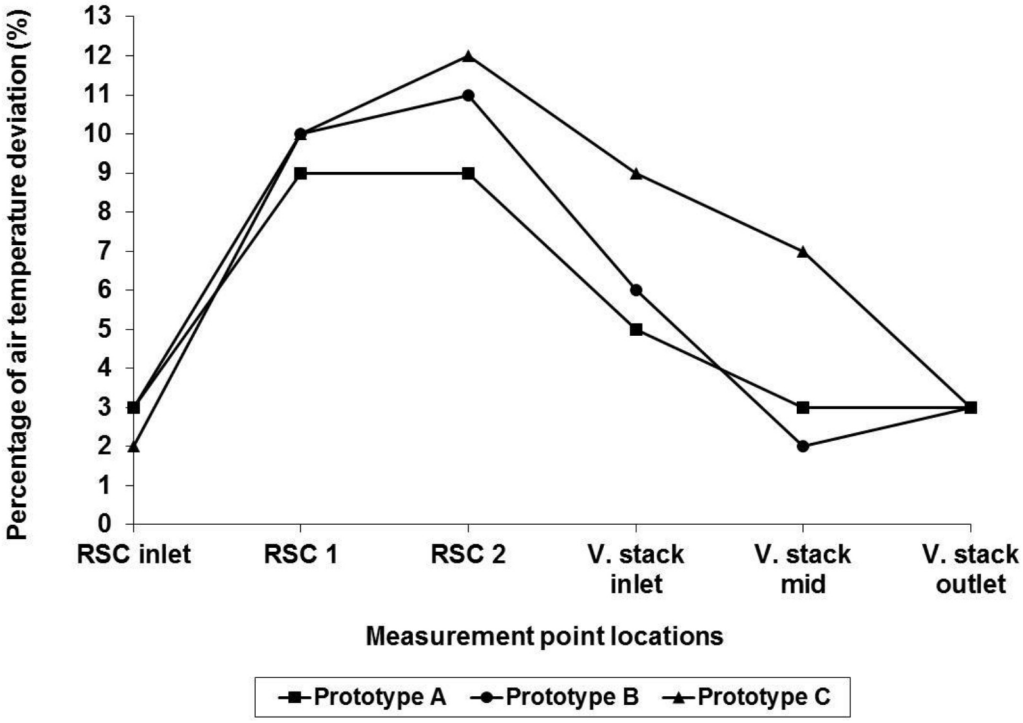

Downloaded from https://prime-pdf-watermark.prime-prod.pubfactory.com/ at 2025-08-29 via free access

FIGURE 7. The average percentage of deviations for air velocity at three measurement point locations for prototype A, B and C.

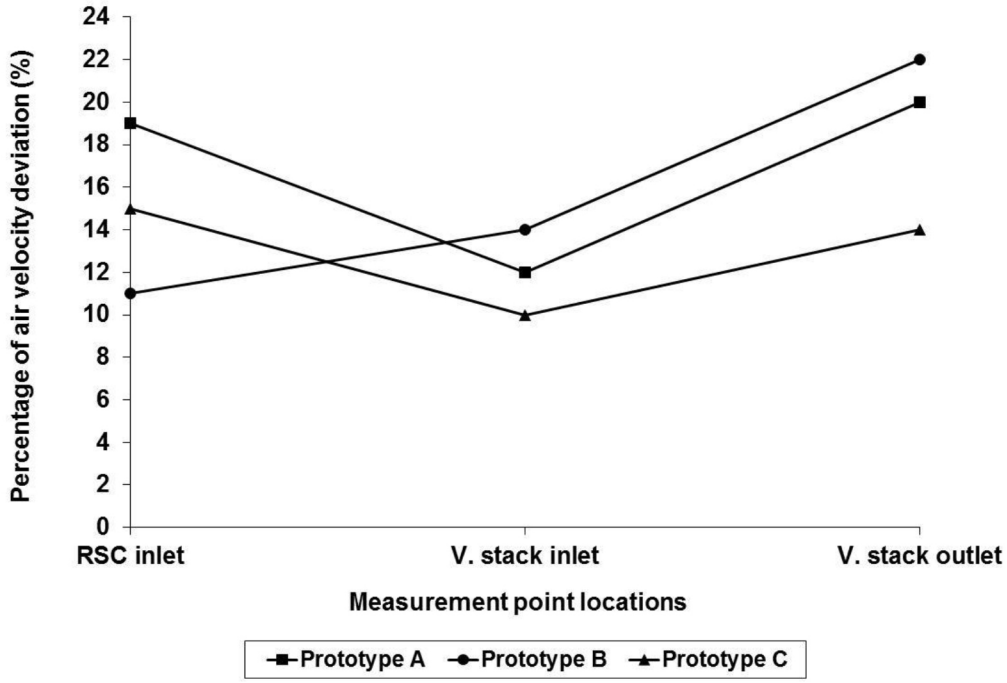

This is because the average deviation for air temperature at six measurement point locations was less than 10%, and the average deviation for air velocity at three measurement point locations was less than 20%. The maximum air temperature deviation was achieved by prototype C, which was 12% at the RSC 2. Meanwhile, the maximum air velocity deviation was obtained by prototype B, which was 22% at the vertical stack outlet.

4. RESULTS AND DISCUSSION

Figure 8 demonstrates the mass flow rate induced by prototype A, B and C for the wind directions from south, southeast and southwest. The x-axis of Figure 8 indicates the solar radiation values from 9 a.m. till 4 p.m. The results showed that the induced mass flow rates at the inlet and middle of the vertical stack had similar profiles. The highest mass flow rate was induced by prototype A, whereas the lowest mass flow rate was obtained by prototype B. On the other hand, the induced mass flow rate at the vertical stack outlet had a different profile. In general, the highest mass flow rate at the vertical stack outlet was induced by prototype C. It was also found that at this location, prototype A had induced a higher mass flow rate compared to prototype B, which was from 9 a.m. to 1 p.m. Meanwhile, starting from 2 p.m. onwards, the results were different, where prototype B induced a higher mass flow rate than prototype A. Prototype A was able to induce the highest mass flow rate of 0.102 kg/s at the vertical stack inlet and mass flow rate of 0.112 kg/s at the middle of the vertical stack for 754 W/m^2 solar irradiation. Figure 8 also shows that the amount of mass flow rate for all the prototypes increased simultaneously with the increase of solar irradiation, except at 2 p.m., where the amount decreased.

The possible explanation for the results derived at the vertical stack outlet of Figure 8 was the presence of wind effects. The wind directions in the simulations were from south,

Downloaded from https://prime-pdf-watermark.prime-prod.pubfactory.com/ at 2025-08-29 via free access

FIGURE 8. Comparisons of mass flow rate induced by prototype A, B and C for the wind direction from south, south-east and south-west.

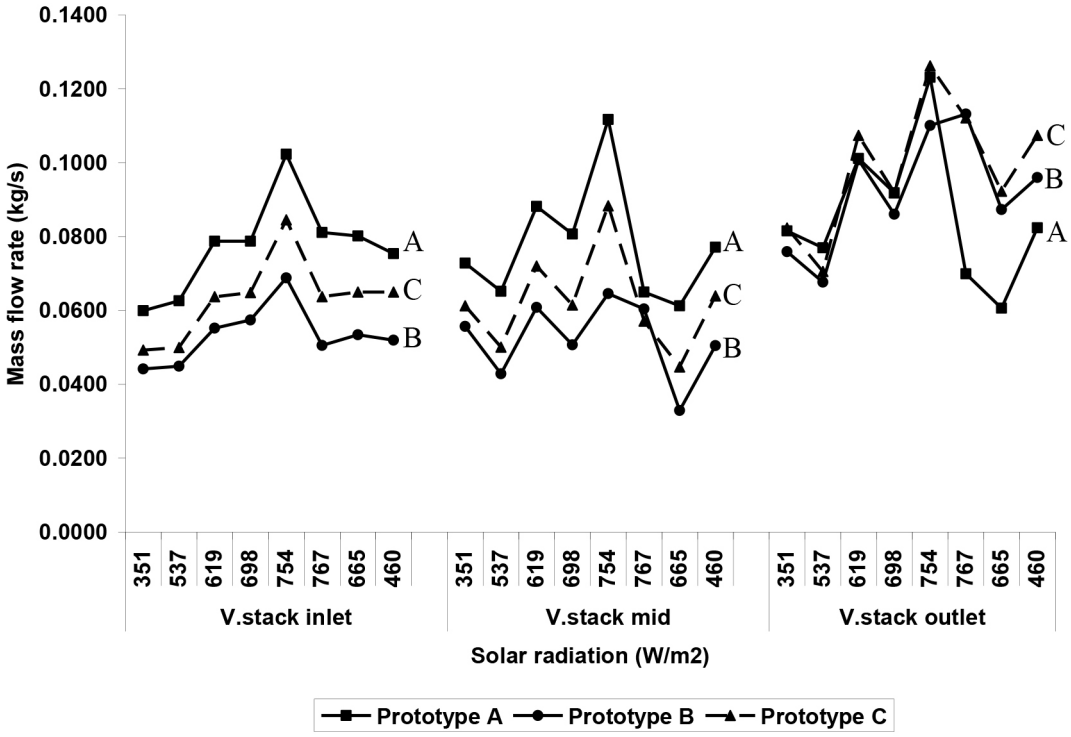

southeast and southwest. The wind effects at prototype A's outlet were found to be the least compared to prototype B and C, as the outlet was located at the leeward side. Prototype B and C had higher wind effects in the evening compared to prototype A, as the wind speed in the evening hours (1 p.m. to 4 p.m.) was higher than the morning and noon hours (9 a.m. to 12 p.m.). Meanwhile, it was found that prototype A induced the highest mass flow rate at the inlet and middle of the stack (Figure 8), due to its opening locations. The inlet openings at the space beneath prototype A were located at the windward side, whereas the outlet opening at the vertical stack was located at the leeward side. The windward location of the inlet and the leeward location of the outlet enabled the wind to enhance the induced mass flow rate (Hunt & Linden, 1999).

Figure 9 depicts the comparisons of mass flow rate induced by the prototypes for the north wind direction. Similarly, the x-axis of Figure 9 indicates the solar radiation values from 9 a.m. till 4 p.m. It is noticeable that prototype A obtained the highest mass flow rate compared to prototype B and C at all locations. Meanwhile, prototype C generally achieved higher mass flow rate than prototype B. However, the mass flow rate in prototype A was due to the wind instead of induced air. The outlet of prototype A was located at the windward side for the north wind direction. This had caused the wind driving force to override the buoyancy force. Hence, downward flow occurred in which the wind entered the prototype through the vertical stack outlet. On the other hand, there was no downward flow inside prototype B and C.

The comparative analyses also demonstrate that besides solar radiation, other factors that influence the induced mass flow rate are the local wind direction, the inlet and outlet positions as well as the outlet design. These factors have to be taken into consideration when developing

Downloaded from https://prime-pdf-watermark.prime-prod.pubfactory.com/ at 2025-08-29 via free access

FIGURE 9. Comparisons of mass flow rate induced by prototype A, B and C for the north wind direction.

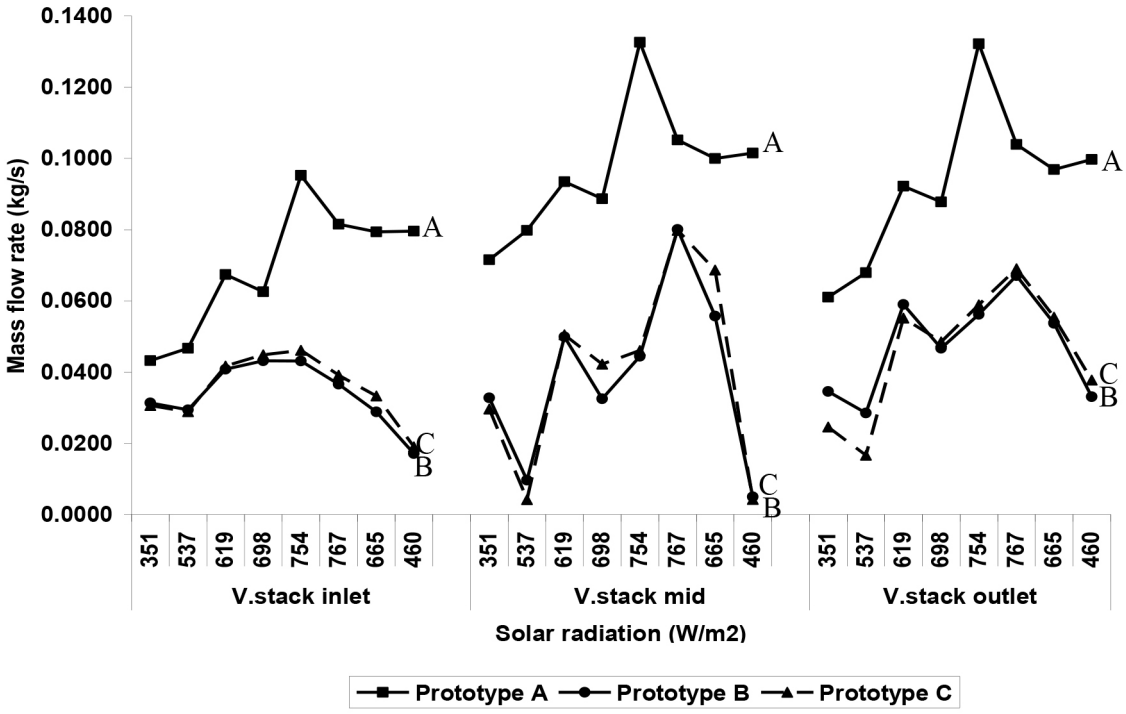

solar induced ventilation. Prototype A, which has an outlet at one side of the wall, is found to be the most appropriate prototype compared to the others, if the prevailing wind is from one direction only. The locations of the inlet at the windward side and the outlet at the leeward side are able to induce high mass flow rate. However, prototype C is found to be more appropriate if the wind is from various directions. This is due to the presence of outlets at both sides of the walls, as well as the obstructions at the outlets that reduce the wind effect. Prototype A is inappropriate as the downward flow might occur if the outlet happens to be at the windward side. Therefore, prototype C is found to be the most appropriate prototype compared to the others for the application in Malaysia due to the various prevailing wind directions. The annual prevailing wind directions recorded by the Subang meteorological station for 33 years (1975–2008) are from the north, northwest and south.

5. CONCLUSIONS

In summary, the investigations indicate that the proposed strategy is able to induce mass flow rate in a hot and humid climate. Although the results indicated that prototype A was able to induce the highest mass flow rate compared to others, it also had the possibility of having downward flow. The downward flow occurred when the outlet of prototype A was located at the windward side. Prototype B and C had no downward flow. The comparisons of these two prototypes show that prototype C was able to induce higher mass flow rate than prototype B. Hence, the study concludes that prototype C, which has obstructions around the outlets, has the most potential as a prototype to enhance the stack effect ventilation in Malaysia. The

Downloaded from https://prime-pdf-watermark.prime-prod.pubfactory.com/ at 2025-08-29 via free access

prevailing wind directions in Malaysia are various. The obstructions function as windbreaks that reduce the wind effect at the vertical stack outlet. The proposed strategy is also expected to be able to enhance the thermal comfort in Malaysian buildings. The increase in mass flow rate will enhance the air change per hour, hence improve the indoor condition of a building. However, the thermal comfort in buildings also depends on other parameters such as the air temperature, the mean radiant temperature and the humidity. This study is limited to the performance of the proposed solar induced ventilation alone, without its application in buildings. Therefore, it is recommended that research investigate the application of the proposed strategy to buildings, by focusing on the indoor thermal comfort. Furthermore, it is also suggested that future studies detail the design of the stack outlet in response to the local prevailing wind.

ACKNOWLEDGEMENT

The authors would like to thank the International Islamic University Malaysia for the endowment of research grant (EDW B 1001-345) that enabled the purchasing of the CFD software.

REFERENCES

Arce, J., Jiménez, M. J., Guzmán, J. D., Heras, M. R., Alvarez, G., & Xamán, J. (2009). Experimental study for natural ventilation on a solar chimney. *Renewable Energy, 34*(12), 2928-2934.

Awbi, H. B. (2003). *Ventilation of Buildings* (Second ed.). London: Spon Press.

Bansal, N. K., Mathur, J., Mathur, S., & Jain, M. (2005). Modeling of window-sized solar chimneys for ventilation. *Building and Environment, 40*(10), 1302-1308.

Bansal, N. K., Mathur, R., & Bhandari, M. S. (1994). A study of solar chimney assisted wind tower system for natural ventilation in buildings. *Building and Environment, 29*(4), 495-500.

Bassiouny, R., & Koura, N. S. A. (2008). An analytical and numerical study of solar chimney use for room natural ventilation. *Energy and Buildings, 40*(5), 865-873.

Boutet, T. S. (1987). *Controlling Air Movement: A Manual for Architects and Builders*. New York: McGraw-Hill Book Company.

Brown, G. Z., & DeKay, M. (2001). *Sun, Wind and Light: Architectural Design Strategies* (Second ed.). New York: John Wiley & Sons, Inc.

Chantawong, P., Hirunlabh, J., Zeghmati, B., Khedari, J., Teekasap, S., & Win, M. M. (2006). Investigation on thermal performance of glazed solar chimney walls. *Solar Energy, 80*(3), 288-297.

Chungloo, S., & Limmeechokchai, B. (2007). Application of passive cooling systems in the hot and humid climate: The case study of solar chimney and wetted roof in Thailand. *Building and Environment, 42*(9), 3341-3351.

Chungloo, S., & Limmeechokchai, B. (2009). Utilization of cool ceiling with roof solar chimney in Thailand: The experimental and numerical analysis. *Renewable Energy, 34*(3), 623-633.

Hamdy, I. F., & Fikry, M. A. (1998). Passive solar ventilation. *Renewable Energy, 14*(1-4), 381-386.

Harris, D. J., & Helwig, N. (2007). Solar chimney and building ventilation. *Applied Energy, 84*(2), 135-146.

Hirunlabh, J., Kongduang, W., Namprakai, P., & Khedari, J. (1999). Study of natural ventilation of houses by a metallic solar wall under tropical climate. *Renewable Energy, 18*(1), 109-119.

Hirunlabh, J., Wachirapuwadon, S., Pratinthong, N., & Khedari, J. (2001). New configurations of a roof solar collector maximizing natural ventilation. *Building and Environment, 36*(3), 383-391.

Hunt, G. R., & Linden, P. P. (1999). The fluid mechanics of natural ventilation—displacement ventilation by buoyancy-driven flows assisted by wind. *Building and Environment, 34*(6), 707-720.

Khedari, J., Boonsri, B., & Hirunlabh, J. (2000b). Ventilation impact of a solar chimney on indoor temperature fluctuation and air change in a school building. *Energy and Buildings, 32*(1), 89-93.

Khedari, J., Hirunlabh, J., & Bunnag, T. (1997). Experimental study of a roof solar collector towards the natural ventilation of new houses. *Energy and Buildings, 26*(2), 159-164.

Khedari, J., Mansirisub, W., Chaima, S., Pratinthong, N., & Hirunlabh, J. (2000a). Field measurements of performance of roof solar collector. *Energy and Buildings, 31*(3), 171-178.

Downloaded from https://prime-pdf-watermark.prime-prod.pubfactory.com/ at 2025-08-29 via free access

Khedari, J., Rachapradit, N., & Hirunlabh, J. (2003). Field study of performance of solar chimney with air-conditioned building. *Energy, 28*(11), 1099-1114.

Kubota, T., Chyee, D. T. H., & Ahmad, S. (2009). The effects of night ventilation technique on indoor thermal environment for residential buildings in hot-humid climate of Malaysia. *Energy and Buildings, 41*(8), 829-839.

Manz, H. (2003). Numerical simulation of heat transfer by natural convection in cavities of facade elements. *Energy and Buildings, 35*(3), 305-311.

Mathur, J., Bansal, N. K., Mathur, S., Jain, M., & Anupma (2006a). Experimental investigations on solar chimney for room ventilation. *Solar Energy, 80*(8), 927-935.

Mathur, J., Mathur, S., & Anupma (2006b). Summer-performance of inclined roof solar chimney for natural ventilation. *Energy and Buildings, 38*(10), 1156-1163.

MentorGraphics (2010). *FloVENT® User Guide-Software Version 9.1*.

Nugroho, A. M. (2007). *Solar Chimney Geometry for Stack Ventilation in Malaysia Terrace House.* Unpublished doctoral dissertation, Universiti Teknologi Malaysia, Johor.

Nugroho, A. M., Hamdan, M., & Ossen, D.R. (2007). A preliminary study of thermal comfort in Malaysia's single storey terraced houses. *Asian Architecture and Building Engineering, 182*, 289-296.

Ong, K. S. (2011). Temperature reduction in attic and ceiling via insulation of several passive roof designs. *Energy Conversion and Management, 52*(6), 2405-2411.

Ong, K. S., & Chow, C. C. (2003). Performance of a solar chimney. *Solar Energy, 74*(1), 1-17.

Puangsombut, W., Hirunlabh, J., Khedari, J., Zeghmati, B., & Win, M. M. (2007). Enhancement of natural ventilation rate and attic heat gain reduction of roof solar collector using radiant barrier. *Building and Environment, 42*(6), 2218-2226.

Punyasompun, S., Hirunlabh, J., Khedari, J., & Zeghmati, B. (2009). Investigation on the application of solar chimney for multi-storey buildings. *Renewable Energy, 34*(12), 2545-2561.

Rahman, A. M. A. (1994). *Design for Natural Ventilation in Low-cost Housing in Tropical Climates.* Unpublished doctoral dissertation, University of Wales College of Cardiff, Cardiff.

Yusoff, W. F. M., Salleh, E., Adam, N. M., Sapian, A. R., & Yusof Sulaiman, M. (2010). Enhancement of stack ventilation in hot and humid climate using a combination of roof solar collector and vertical stack. *Building and Environment, 45*(10), 2296-2308.

Downloaded from https://prime-pdf-watermark.prime-prod.pubfactory.com/ at 2025-08-29 via free access